Rivista Italiana di Paleontologia e Stratigrafia
(*Research in Paleontology and Stratigraphy*)
vol. 122(3): 165-184. **November 2016**

CAMPANIAN CALCAREOUS NANNOFOSSIL BIOSTRATIGRAPHY OF EASTERN KOPPEH-DAGH BASIN (NORTH EAST OF IRAN), TETHYAN REALM

FARIBA FOROUGHI [1*], SILVIA GARDIN [2] & ANOSHIRAVAN LOTFALI KANI [3]

[1*]Corresponding author. Exploration Directorate, National Iranian Oil Company, Seoul St., NE Sheikh Bahaei Sq., 1994814695, Tehran, Iran. E-mail: fariba.foroughi86@gmail.com
[2]Centre de recherche sur la Paléobiodiversité et les Paléoenvironnements, UMR CNRS 7072, Université Pierre et Marie Curie Paris 06, 4, place Jussieu, 75252 Paris cedex 05, France.
[3]Geology Department, Earth Sciences Faculty, Shahid Beheshti University, 1983963113, Daneshjoo Blvd., Evin, Tehran, Iran.

To cite this article: Foroughi F., Gardin S. & Lotfali Kani A. - Campanian calcareous nannofossil biostratigraphy of Eastern Koppeh-Dagh Basin (Northeast of Iran), Tethyan Realm. *Riv. It. Paleontol. Strat.,* 122(3): 165-184.

Keywords: Abtalkh Formation, Calcareous nannofossil, Campanian, Iran, Koppeh-Dagh Basin.

Abstract. Tethyan calcareous nannofossil assemblages have been recorded from three sections of the Abtalkh Formation including the type section at Abtalkh village and two others (Padeha and Jalilabad) in the east Koppeh-Dagh Basin, north east of Iran. The formation studied is expanded with a thickness of up to 1770 m at the type locality in the middle of eastern Koppeh-Dagh spanning biozones UC15b^{TP} to UC16 while in the Padeha (973.5 m thick) in east and Jalilabad (1316 m thick) section in the west the formation spans biozones UC14d^{TP}–UC15a^{TP} to of UC16. The zonation erected indicates an age of early–latest Campanian for the Abtalkh Formation. The recorded assemblages are of low-latitude to intermediate forms suggesting placement of the Koppeh-Dagh Basin in low to intermediate latitudes during Campanian.

Introduction

The Koppeh–Dagh Basin stretches NW–SE east of the Caspian Sea north east of Iran, Turkmanistan, and Afghanistan. Sedimentation was continuous from Jurassic through the Neogene (Berberian & King 1981; Afshar-Harb 1994) depositing ca. 6500 m of shale, marl and limestone (Afshar-Harb 1994). The Iranian part of the basin is located between longitudes 36° 00' - 38° 16' E and latitudes 54°00' - 61°41' N (Fig. 1A).

As the Koppeh-Dagh Basin is an important hydrocarbon oil field, it has been considered as a target for a number of multidisciplinary studies (paleontological, sedimentological and structural–geological) by the National Iranian Oil Company. Biostratigraphic and sedimentologic studies have been made on the basin's Cretaceous strata (Kalantari 1969; Afshar-Harb 1969, 1979, 1994; Seyed-Emami & Aryai 1981; Raisossadat & Moussavi-Harami 2000; Hadavi 2004; Hadavi & Notghi Moghadam 2010; Vahidinia & Sadeghi 2011; Mahanipour et al. 2011 and Notghi Moghadam et al. 2013).

The Abtalkh Formation is one of the thickest upper Cretaceous rock units in the Koppeh-Dagh Basin (Stocklin & Setudehnia 1991) and consists of green to gray marls, green siltstones and gray silty marls. This formation conformably overlies the upper most chalky limestone beds of the Abderaz Formation which contains mainly yellow, green to gray marls and three to four white to yellow thick chalky limestone beds and is overlain by the Nayzar Formation, which consists of green to gray siltstone and sandstone, and yellow limestone (Afshar-Harb 1994).

Calcareous nannofossils and foraminifera have provided different ages, ranging from Santonian to Maastrichtian for the formation. For example Kalantari (1969), Afshar-Harb (1994) and Ahmadi (2011) provided an age of Santonian to Masstrichtian while, Niyazi (2011) reported Campanian for the formation based on foraminifera. On the other hand, based on calcareous nannofossils, Hadavi (2004), suggested Santonian–early Maastrichtian age for the formation, while Hadavi & Notghi Moghadam (2010) reported Santonian–Campanian for the upper part of Abderaz and lower part of Abtalkh Formation in eastern Koppeh-Dagh. Few studies have been carried out on the nannofossil biostratigraphy of Upper Cretaceous sediments

Received: March 6, 2016; accepted: September 25, 2016

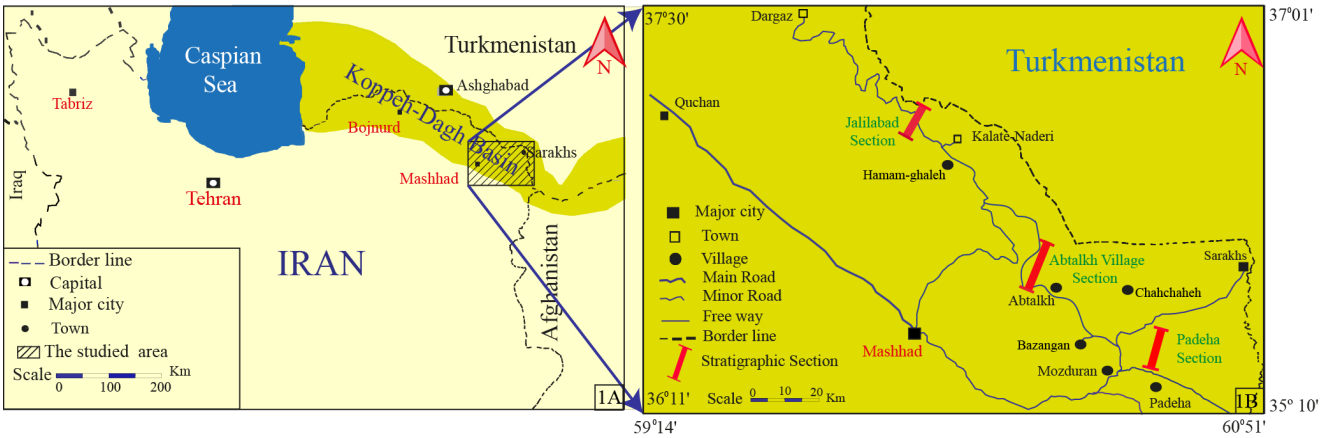

Fig. 1 - A) Extension of the Koppeh-Dagh Basin and studied area (modified after Berberian & King 1981); B) the three stratigraphic sections in the eastern Koppeh-Dagh and road map of the studied area (modified after Afshar-Harb 1982 and Google map 2015).

at different localities of the Iranian Koppeh-Dagh Basin (Hadavi 2004; Hadavi & Notghi Moghadam 2010).

The discrepant given ages present the need for a better stratigraphic constraint for the Cretaceous sedimentary successions and the potential of rich and abundant calcareous nannofossil assemblages has prompted a detailed reinvestigation of the Abtalkh Formation in the area.

The purpose of this study is to establish an age for the formation in this part of the basin based on calcareous nannofossil biostratigraphy and to evaluate the applicability of the well-established schemes of the Tethyan realm.

Material and methods

The studied sections are located in the eastern Koppeh-Dagh Basin. The Padeha section is 135 km to the south east of Mashhad City, near Dusti Dam at 36° 06' 47" N and 60°44' 00" E. The second section studied, the Abtalkh village, is located 170 km to the north east of Mashhad at 36° 28' 62" N and 60° 23' 99" E. The third section, at Jalilabad is located 142 km southwest of Kalate-Naderi, north of Mashhad City at 36° 59' 58" N and 59° 41' 41" E (Fig. 1B). The distance between the sections is approximately 50 to 80 km.

A total of 956 samples were collected from the three sections (250 samples from Padeha, 446 samples from Abtalkh village and 210 samples from Jalilabad). Sampling density varied from 3 to 5 m and the samples were prepared using the gravity settling technique (Bown 1998).

Nannofossils were analysed using an Axioplan Imaging II Zeiss Light Microscope (LM) at a magnification of X1570. All photographic images were taken in either cross-polarized light (XPL) or bright field (BF), plane light without a single polariser. Five to seven traverses (approximately 1000 fields of view=FOV) were considered to observe the First Occurrence (FO) and the Last Occurrence (LO) of taxa. Semi–quantitative counts were determined as follows: Abundant (A) more than 10 specimens observed in a field of view; Common (C) one to 10 specimens in each field of view; Few (F) one specimen observed in 10 fields of view; Rare (R) only one specimen in 11 to 100 fields of view; and Single (S) only one specimen during the investigation.

Preservation of calcareous nannofossils for these sections was described applying the methods of Roth (1978) and Watkins (2007) varied from Good (G), Moderate (M) to Poor (P).

Calcareous nannofossil images were taken using cross polarized light (XPL) and reported in Plates 1 to 7 (FPB= Padeha, FKB= Abtalkh village and FJB= Jalilabad).

Biostratigraphy

Calcareous nannofossil biozonations of the Campanian–Maastrichtian interval have been proposed by Sissingh (1977); Roth (1978); Perch-Nielsen (1985) and Burnett (1998). In this study the stratigraphic zonation developed by Burnett (1998) for the Tethyan realm was applied. Bibliographic references for the determined taxa are given in Perch-Nielsen (1985), Bown (1998) and Lees & Bown (2005).

Based on bioevents, zones and subzones were determined as represented in Plates 1-7 and are described as follows:

1. Subzone UC14d^{TP}–UC15a^{TP}

Definition: This subzone is marked by the FO of *Ceratolithoides verbeekii* to FO of *Ceratolithoides aculeus*. The UC14d^{TP} is recognized by the FO of *C. verbeekii* to FO of *Monomarginatus quaternarius* and UC15a^{TP} is identified by the FO of *M. quaternarius* to FO of *C. aculeus*. The FO of *Staurolithites mielnicensis* occurs in the upper part of the UC14d^{TP}. This subzone shows the upper part of UC14d^{TP} to UC15a^{TP}.

Age: early Campanian.

This study: In the sections studied the *M. quaternarius* was not recorded. The other markers *S. mielnicensis, Broinsonia parca constricta* and *Reinhardtites anthophorus* were all recorded within the subzone. This merged biozone was only recognized in Padeha and Jalilabad sections.

2. Subzone UC15b^{TP}

Definition: This subzone is equivalent of Zone CC20 of Sissingh (1977). This subzone is marked by the FO of *C. aculeus* at the base and FO of *Uniplanarius sissinghii* at the top.

Age: late Early Campanian.

This Study: This subzone is present in all three studied sections. The FOs of *Rusinolithus magnus*, *Microrhabdulinus ambiguus* (curved spine) and some intermediate forms between *Reinhardtites anthophorus* and *Reinhardtites levis* are all observed in this biozone.

3. Subzone UC15c^{TP}

Definition: This subzone is equivalent of Zone CC21 of Sissingh (1977) and is defined by the FO of *Uniplanarius sissinghii* at the base and the FO of *Uniplanarius trifidus* at the top.

Age: Approximately early Late Campanian.

This study: This subzone is recognized in all three studied sections.

4. Subzone UC15d^{TP}

Definition: This subzone is defined by the FO of *U. trifidus* to FO of *Eiffellithus parallelus*.

Age: early Late Campanian.

This study: This subzone is existed in all three studied sections.

5. Subzone UC15e^{TP}

Definition: This subzone is defined by the FO of *E. parallelus* to the LO of *Eiffellithus eximius* (Burnett 1998) whose LO is equivalent to the LO of *R. anthophorus* (Perch-Nielsen 1985; Burnett 1998).

Age: early Late to Late Campanian.

This Study: This subzone was recorded in all three sections studied. The FOs of *Quadrum svabenickae* and *Monomarginatus quaternarius* and LOs of *R. magnus* and *M. ambiguus* (curved spines) are also found in this subzone. Subzones UC15d^{TP} and UC15e^{TP} are equivalent of CC22 of Sissingh (1977).

6. UC16 Zone

Definition: This zone is defined as the interval from the LOs of *E. eximius* and/or *R. anthophorus* (Perch-Nielsen 1985; Burnett 1998) to the LO of *B. parca constricta* and is equivalent to Zone CC23a of Sissingh (1977).

Age: latest Campanian.

This Study: This zone has been recorded in all three sections studied. Moreover, *Tranolithus orionatus* (=*Tranolithus phacelosus*), *B. parca constricta*, *U. trifidus* and *R. levis* are recorded in the uppermost layers of Abtalkh Formation.

Discussion

All the studied sections contain abundant and moderate to well-preserved calcareous nannofossil assemblages that allowed application of the UC^{TP} (Tethyan Province) Zonation of Burnett (1998). It was not always possible to identify all the biozones and subzones due to the absence of given stratigraphic markers. Consequently a merged interval was introduced for the basal part of the Padaha and Jalilabad sections. Other secondary bio-horizons with probable regional significance were also identified. The nannofossil events detected in the studied sections are reported in Tabs 1, 2 and 3.

The subzones UC14d^{TP} and UC15a^{TP} are generally differentiated by the presence of *M. quaternarius*. As in the existing literature, this species was neither recorded from the Abderaz nor from the Abtalkh strata in this study forcing the authors to introduce the merged interval of UC14d^{TP}–UC15a^{TP}and placing the upper Abderaz and lower Abtalkh Formation at Padeha and jalilabad sections in this interval. The first samples of the Abtalkh Formation contain the marker species such as *C. verbeekii*, *S. mielnicensis*, *B. parca constricta* and *R. anthophorus* confirming the UC14d^{TP} for the base of the formation in Padeha and Jalilabad sections. This merged interval attains a thickness of about 1.4 m in Padeha and 54.6 m in Jalilabad sections. The base of the Abtalkh village section begins with UC15b^{TP}which spans the upper Abderaz and the basal Abtalkh strata.

The UC15b^{TP} is defined as the interval between the FO of *C. aculeus* to the FO of *U. sissinghii*. This subzone attains a thickness of about 214 m in Padeha, 83.2 m in Abtalkh village and 54 m in Jalilabad sections.

The FOs of *Rucinolithus magnus* and *M. ambiguus* (curved spine), markers for early to late Campanian,

Nannofossil bio-events in Padeha section	Thickness (m)	Sample No. (FPB)
LO of *Reinhardtites anthophorus*	985	FPB 354
LO of *Eiffellithus eximius*	983.3	FPB 353
LO of *Rucinolithus magnus*	981.8	FPB 348
LO of *Micorhabdulinus ambiguus* (curved spine)	870	FPB 345
FO of *Eiffellithus parallelus*	542.1	FPB 312
FO of *Reinhardtites levis*	466.5	FPB 298
FO of *Uniplanarius trifidus*	272.2	FPB 242
FO of *Uniplanarius sissinghii*	229.9	FPB 219
FO of *Micorhabdulinus ambiguus* (curved spine)	182	FPB 193
FO of *Rucinolithus magnus*	47.8	FPB 135
FO of *Ceratolithoides aculeus*	15.9	FPB 112
FO of *Broinsonia parca constricta*	Base of section (0)	FPB 100
FO of *Calculites ovalis*	Base of section (0)	FPB 100
FO of *Staurolithites mielnicensis*	Base of section (0)	FPB 100

Tab. 1 - Calcareous nannofossils bio-events in Abtalkh Formation in Padeha section of eastern Koppeh-Dagh Basin.

Nannofossil bio-events in Abtalkh village section	Thickness (m)	Sample No. (FKB)
LO of *Reinhardtites anthophorus*	1668.2	FKB 517
LO of *Eiffellithus eximius*	1620.2	FKB 501
LO of *Rucinolithus magnus*	1488.9	FKB 469
LO of *Micorhabdulinus ambiguus* (curved spine)	1350	FKB 429
FO of *Eiffellithus parallelus*	567.1	FKB 177
FO of *Uniplanarius trifidus*	454.2	FKB 159
FO of *Reinhardtites levis*	389.2	FKB 149
FO of *Uniplanarius sissinghii*	83.2	FKB 125
FO of *Micorhabdulinus ambiguus* (curved spine)	73.2	FKB 120
FO of *Rucinolithus magnus*	45.2	FKB 112
FO of *Ceratolithoides aculeus*	20.3	FKB 109
FO of *Broinsonia parca cnstricta*	Base of section (0)	FKB 100
FO of *Broinsinia parca parca*	Base of section (0)	FPB 100
FO of *Calculites ovalis*	Base of section (0)	FPB 100
FO of *Staurolithites mielnicensis*	Base of section (0)	FPB 100

Tab. 2 - Calcareous nannofossils bio-events in Abtalkh Formation in Abtalkh village section of eastern Koppeh-Dagh Basin.

Nannofossil bio-events in Jalilabad section	Thickness (m)	Sample No. (FJB)
LO of *Eiffellithus eximius*	1318.9	FJB 290
LO of *Reinhardtites anthophorus*	1318.9	FJB 290
LO of *Micorhabdulinus ambiguus* (curved spine)	1299.3	FJB 275
LO of *Rucinolithus magnus*	1228	FJB 265
FO of *Eiffellithus parallelus*	755.8	FJB 215
FO of *Uniplanarius trifidus*	570.8	FPB 194
FO of *Reinhardtites levis*	533.4	FJB 189
FO of *Micorhabdulinus ambiguus* (curved spine)	385	FJB 146
FO of *Uniplanarius sissinghii*	128.8	FJB 137
FO of *Rucinolithus magnus*	124	FJB 124
FO of *Ceratolithoides aculeus*	74.8	FJB 121
FO of *Staurolithites mielnicensis*	Base of section (0)	FJB 100
FO of *Ceratolithoides. verbeekii*	Base of section (0)	FJB 100
FO of *Broinsonia parca parca*	Base of section (0)	FJB 100
FO of *Broinsonia parca constricta*	Base of section (0)	FJB 100

Tab. 3 - Calcareous nannofossils bio-events in Abtalkh Formation in Jalilabad section of eastern Koppeh-Dagh Basin.

are regognized in subzone UC15b^{TP} at Padeha and Abtalkh village sections. But the FO of *M. ambiguus* (curved spine) is found in the subzone UC15c^{TP} at Jalilabad section due to poor preservation or slide prepration technique. Intermediate forms between *R. anthophorus* and *R. levis* were recorded before presence of true *R. levis* in this subzone (Pl. 2., figs 4, 8). Similar intermediate forms were reported from Contessa Highway and Bottaccione sections of Tethyan realm in Gubbio area of Italy (Gardin et al. 2012) and in the Indian Ocean (Thibault et al. 2012).

Subzone UC15c^{TP} is much thicker in Jalilabad (442 m) than in Abtalkh village (371 m) and Padeha (42.3 m) sections while, subzone UC15d^{TP} reaches its greatest thickness in Padeha (269.9 m) where it is much thicker than the Abtalkh village (112.9 m) and Jalilabad (185 m). Although *Retecapsa schizobrachiata* is common in low latitude sections (Bown 1998), this species recorded rarely in this biozone. Also, two distinct forms of *U. trifidus*, one with wide and short rays, which appears first, and another with narrow and tall rays appearing in upper strata (Pl. 7, Figs 3, 4, 8) were recorded in this subzone. *Uniplanarius trifidus* is a warm water form recorded from tropical low to intermediate paleolatitudes (Roth 1978; Erba et al. 1992; Burnett et al. 2000; Thibault et al. 2012).

Subzone UC15e^{TP} is thicker in the Abtalkh village section (1053 m) than in Padeha (441.2 m) and Jalilabad (563.1 m). In this subzone, the FO of *Q. svabenickae* occurs in the lower middle part of the zone and the FO of *Monomarginatus quaternarius* follows shortly. LOs of *C. ovalis*, *R. magnus*, *R. anthophorus* and *M. ambiguus* (curved spine) [at low–paleolatitudes, Bown 1998], *E. eximius*, *L. grillii,* and *B. parca parca* were recorded in all three sections. The LO of *C. ovalis* is earlier than LO of *R. magnus* and shortly follows LOs of *L. grillii* and *M. ambiguus* (curved spine) (Tabs 1, 2 & 3 and Figs 2, 3 & 4). It seems that the highest sedimentation rate of the Abtalkh Formation was occurring in this biozone during this time due to high thickness of this subzone in three sections.

Zone UC16 was identified in all three studied sections based on the co-occurrence of *B. parca constricta*, *T. orionatus* and *R. levis* in uppermost strata of the Abtalkh and extends upwards to the Neyzar Formation. This zone in Abtalkh village (158 m) is thicker than in Padeha (4.6 m) and Jalilabad (17.4 m) sections.

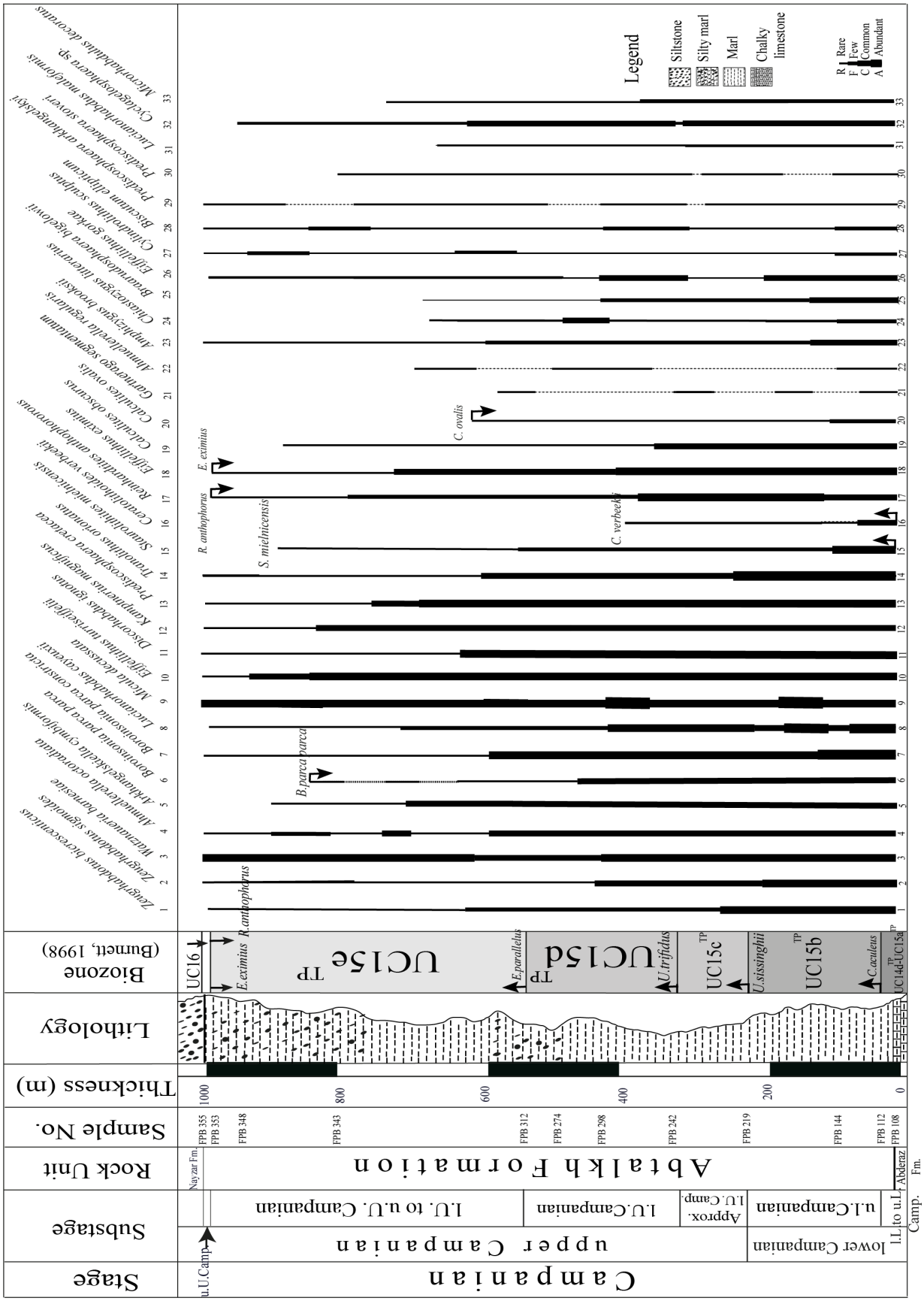

Fig. 2a - Distribution of calcareous nannofossils in the Padeha stratigraphic section (continue).

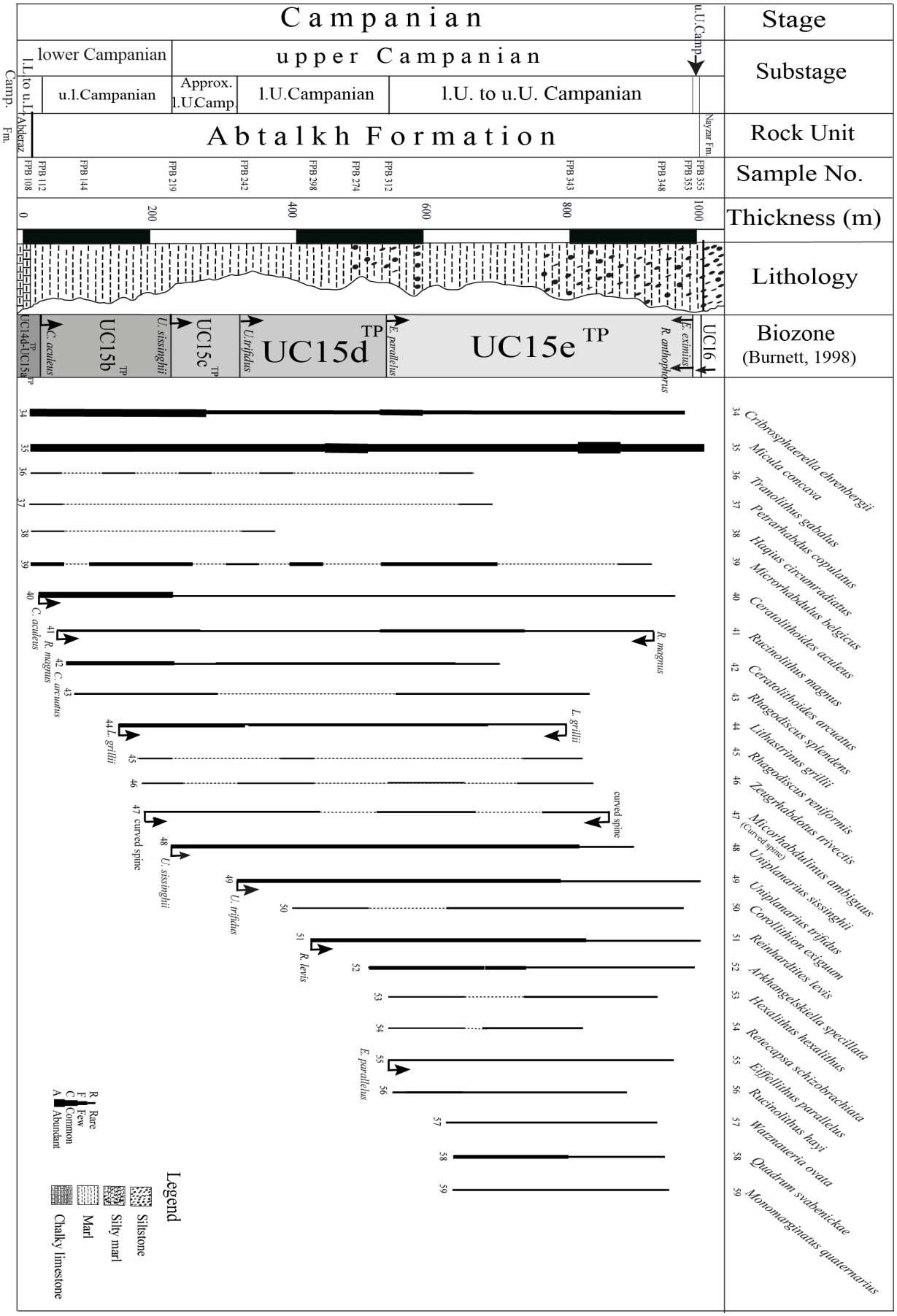

Fig. 2b - Distribution of calcareous nannofossils in the Padeha stratigraphic section.

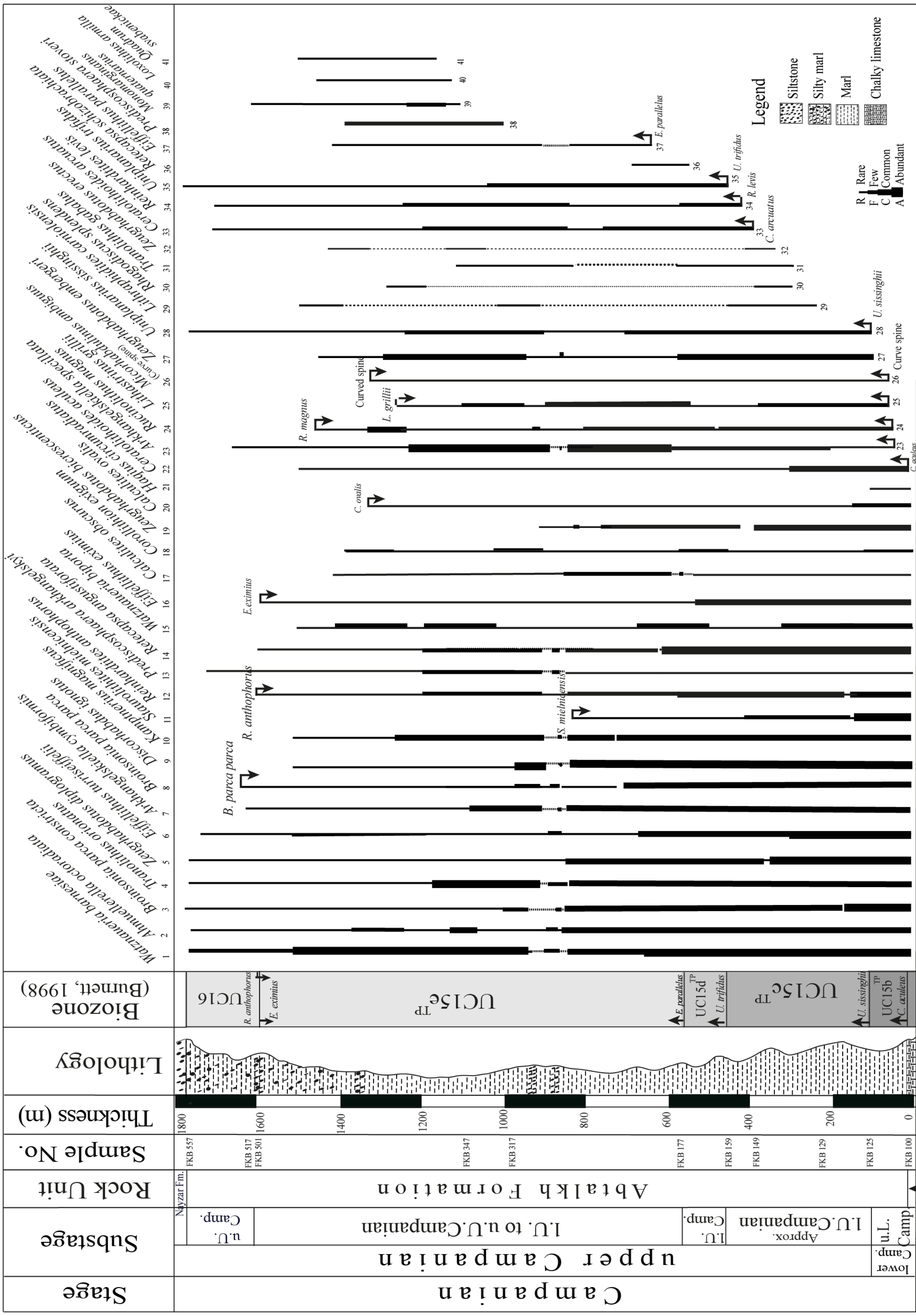

Fig. 3 - Distribution of calcareous nannofossils in the Abtalkh village stratigraphic section.

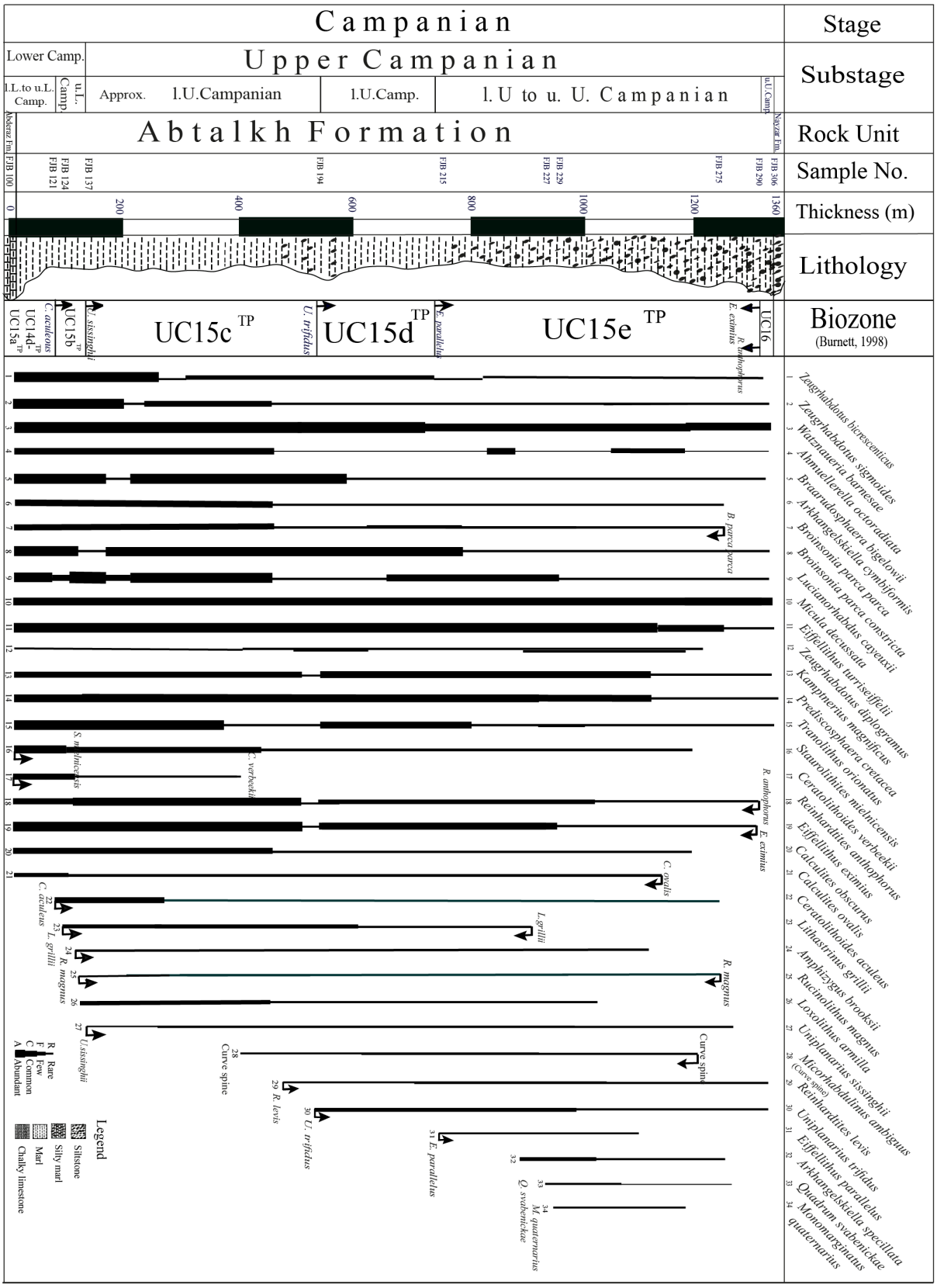

Fig. 4 - Distribution of calcareous nannofossils in the Jalilabad stratigraphic section.

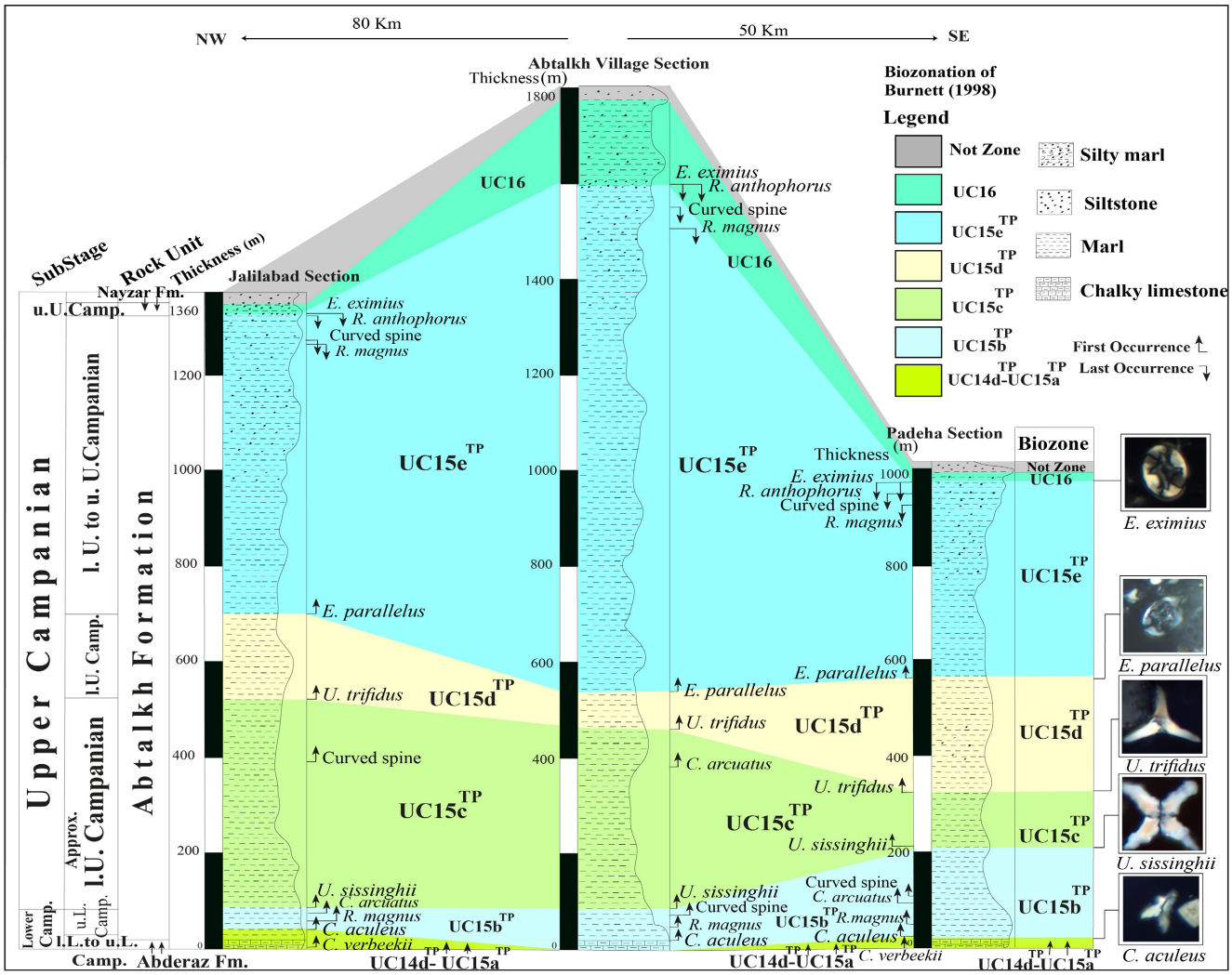

Fig. 5 - Correlation between the three studied sections in the eastern Koppeh-Dagh Basin.

Based on calcareous nannofossil assemblages recorded here, the age of the Abtalkh Formation in the eastern Koppeh-Dagh Basin is early to latest Campanian. The greater thickness of the formation at the Abtalkh village section indicates thickening of the formation in the middel of the eastern Koph-Dagh Basin (Fig. 5).

Diversity of nannofossil assemblages is high in all studied sections and decreased from base to top of the sections (Figs 2, 3 & 4). The changes in diversity are in accord with those occurring in lithology from marl to silty marls. At the same time forms with high degree of resistance against solution such as *Micula decussata*, *Watzenueria barnesiae* and *Ceratolithoides* spp. increase upwards the sections.

The authors have also compared and correlated their biostratigraphy with the existing zonation on the Abtalkh Formation (Hadavi 2004) and with the standard zonations published by Tercis Les Landes (SW France), GSSP of Campanian-Maastrichtian (Gardin et al. 2001) and of Roth (1978), Sissingh (1977), Perch-Nielsen (1985) and Burnett (1998) for the Tethyan realm. Except for an interval at the base of the sections where the index species for UC14d^{TP} and UC15a^{TP} were not recorded and therefore a merged interval is introduced, the zonation for the rest of the Abtalkh Formation is identical with these standard schems presented by the aforementioned authors (Fig. 6).

In Fig. 6 the standard zonation schemes of Tethyan province in Santonian to early Maastrichtian and biozonation established for the studied sections in eastern Koppeh-Dagh Basin is shown.

The Koppeh-Dagh Basin remained in Tethyan realm with high abundance of warm water taxa like *Watznaueria* spp., *Ceratolithoides* spp., *Micula decussata* and presence of *U. trifidus and S. schizobrachiata* and low abundance or absence of high latitude and cold taxa like *Gartnerago segmentatum*, *Kamptnerius magnificus*, *Biscu-*

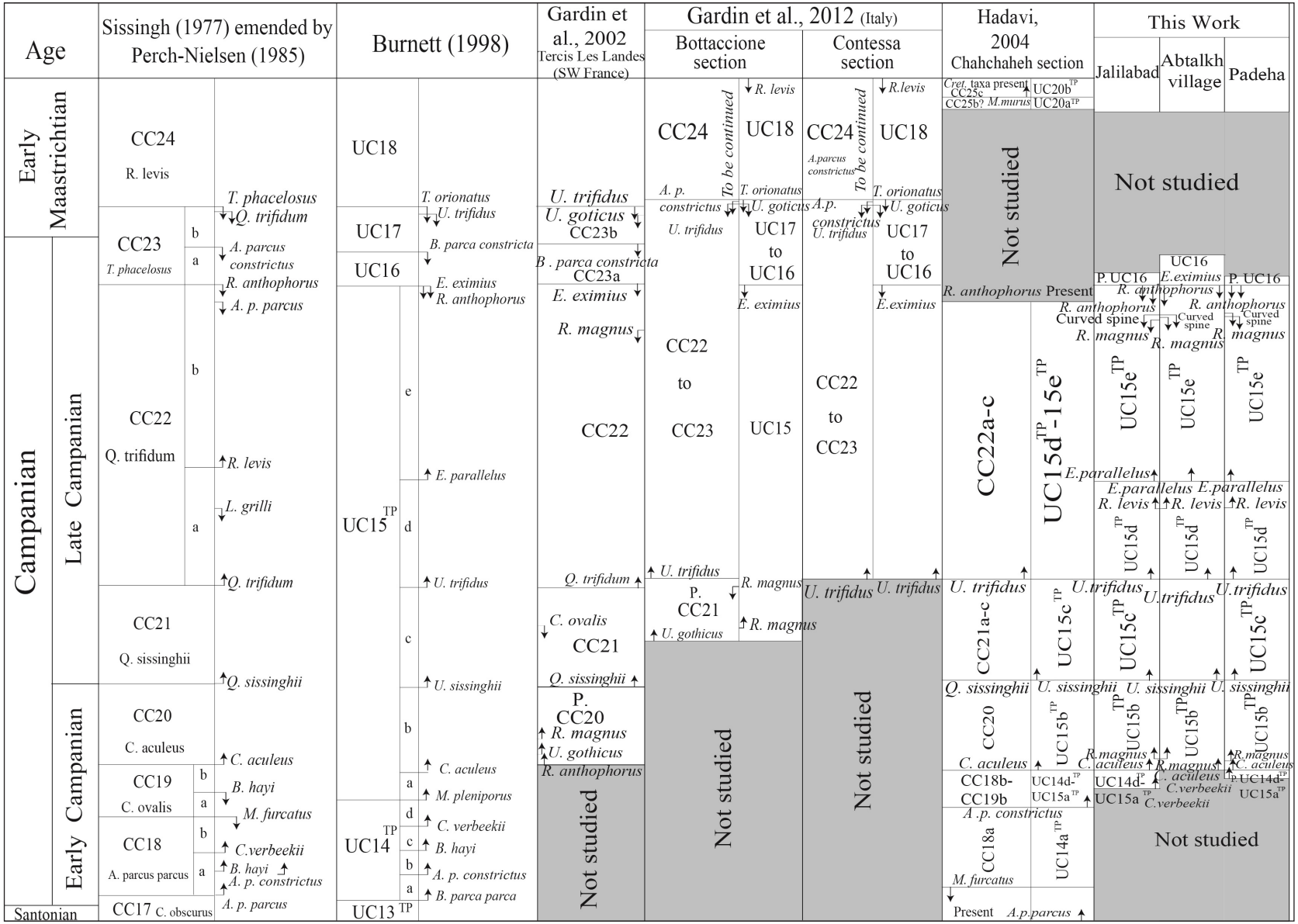

Fig. 6 - Comparison between Santonian to early Maastrichtian calcareous nannofossil standard zonation schemes of the Tethyan province. The biozonation established for the studied sections in eastern Koppeh-Dagh Basin is provided for comparison.

tum magnum in studied sections (see the Figs 2, 3 & 4). The data of studied sections showed that the Koppeh-Dagh Basin was located in low to intermediate paleolatitudes and followed biozonation of Tethyan domain.

Conclusion

From bottom to the top of the Abtalkh Formation, part of UC14d^{TP}–UC15a^{TP}, UC15b^{TP}, UC15c^{TP}, UC15d^{TP} subzones and UC16 biozone were identified however, the UC14d^{TP}–UC15a^{TP} subzone was not recognized in the Abtalkh village section. The biozonation scheme established for the Tethyan realm is fully applicable for the Abtalkh Formation and all zonal and sub-zonal events were recognized. The age of the Abtalkh Formation is estimated to be of early to latest Campanian. Presence of low-latitude forms and absence or rareness of high-latitude forms indicates that the basin was located in low to intermediate latitudes.

Acknowledgements. Financial support from the Ministry of Science, Research and Technology of Iran is appreciated. Special thanks go to two anonymous reviewers who kindly reviewed the versions of the manuscript and gave many comments that greatly improved quality of this paper. Dr. Vahidinia of the Ferdowsi University of Mashhad and Dr. Thibault of the Copenhagen University are appreciated for their help provided during the course of this study. Dr. Ghasemi-Nejad from University of Tehran is thanked for helping edition of the manuscript and Dr. Raffi, editor of the Rivista Italiana di Paleontologia e Stratigrafia Journal is thanked for helpful comments on the versions of the manuscript.

REFERENCES

Afshar-Harb A. (1969) - History of oil exploration and brief description of the geology of the Sarakhs area and the anticline of Khangiran. *Bull. Iranian Petrol. Inst., Tehran*, 37: 86-94.

Afshar-Harb A. (1979) - The stratigraphy, tectonics and petroleum geology of the Koppeh-Dagh region, northern Iran, Unpublished Ph.D. thesis, Imperial College of Science and Technology, London: 316.

Afshar-Harb A. (1982) - Geological quadrangle map of Sarakhs, 1:250,000 scale (one sheet). Exploration and Production, NIOC, Tehran.

Ahmadi M. (2011) - Lithostratigraphy and biostratigraphy of Abtalkh Formation based on foraminifera in Padeha stratigraphical section (south east of Mashhad). M.Sc. thesis in Ferdowsi University of Mashhad, Iran: 270 [In Persian].

Afshar-Harb A. (1994) - Treatise on the Geology of Iran; Geology of the Koppeh–Dagh. Geol. surv. Iran, 11. Tehran, 275 pp. [In Persian].

Berberian M. & King G.C.P. (1981) - Toward a palaeogeography and tectonic evolution of Iran. *Can. J. Earth Sci.* 18: 210-265.

Bown P.R (1998) - Calcareous Nannofossil Biostratigraphy. *British Micropaleontolo. Soc. Pub. Series*. Chapman & Hall, London, 328 pp.

Burnett J.A. (1998) - Upper Cretaceous. In: Bown P.R. (Ed.) - Calcareous Nannofossil Biostratigraphy: 132-199. Chapman and Hall, Cambridge.

Burnett J.A., Young J.R. & Bown P.R. (2000) - Calcareous nannoplankton and global climate change. Biotic response to global change: 35-50. Cambridge University Press.

Erba E., Castradori D., Guasti G. & Ripepe M. (1992) - Calcareous nannofossils and Milankovitch cycles: the example of the Albian Gault Clay Formation (southern England). *Palaeogeogr., Palaeoclimatol., Palaeoecol.,* 93: 47-69.

Gardin S., Odin G.S., Bonnermaison M., Melinte M., Monechi S. & Von Salis K. (2001) - Results of the cooperative study on the calcareous nannofossils across the Campanian–Maastrichtian boundary at Tercis les Bains (Landes, France). In: Odin G.S. (Ed.) - The Campanian–Maastrichtian Boundary: 293-309. Elsevier Science B.V.

Gardin S., Galbrun B., Thibault N., Coccioni R. & Premoli Silva I. (2012) - Bio-magnetochronology for the upper Campanian–Maastrichtian from the Gubbio area, Italy: new results from the Contessa Highway and Bottaccione sections. *Newsl. Stratigr.,* 45(1):75-103.

Gradstein F.M., Ogg J.G., Schmitz M.D. & Ogg G. (2012) - Updated Geological time scale, 2006. Elsevier Science, Publication 1, 1144 pp.

Hadavi F. (2004) - Calcareous nannofossils from the Abtalkh Formation (Campanian-Maastrichtian), Kopet-Dagh range, NE Iran. *J. Nannoplankton Res.*, 26(1): 63-68.

Hadavi F. & Notghi Moghadam M. (2010) - Calcareous nannofossils from chalky limestone of upper Abderaz Formation and lower part of Abtalkh Formation in the Kopet-Dagh range NE Iran. *Arab. J. Geosci.,* 10.1007/s12517–009–0106–5.

Kalantari A. (1969) - Foraminifera from the Middle Jurassic-Cretaceous successions of Koppeh-Dagh region (NE-Iran). Ph.D. thesis, University of London, England.

Lees J.A. & Bown P.R. (2005) - Upper Cretaceous calcareous nannofossil biostratigraphy, ODP Leg 198 (Shatsky Rise, northwest Pacific Ocean). In: Bralower T.J., Premoli Silva I. & Malone M.J. (Eds) - Project ODP, Science Results, 198: 1-60.

Mahanipour A., Mutterlose J.L., Kani A. & Adabi M.H. (2011) - Palaeoecology and biostratigraphy of early Cretaceous (Aptian) calcareous nannofossils and the δ^{13} Carbon isotope record from NE Iran. *Cretaceous Res.*, 32: 331-356.

Niyazi M. (2011) - Lithostratigraphy and biostratigraphy of Abtalkh Formation based on foraminifera in Ghare-su stratigraphical section (West of Kalat). M.Sc. thesis in Ferdowsi University of Mashhad, Iran: 260 [In Persian].

Notghi Moghadam M., Hadavi F. & Moheghi M.A. (2013) -

Nannostratigraphy and paleoenvironmental study of the lower boundary of the Kalat Formation in East and West of Kopet-Dagh, Northeast Iran. *Geopersia,* 3/2: 99-116.

Perch-Nielsen K. (1985) - Mesozoic Calcareous Nannofossils. In: Bolli H.M., Saunders J.B. & Perch-Nielsen K. (Eds) - Plankton stratigraphy: 329-426. Cambridge Earth Science Series, Cambridge University Press.

Raisossadat N. & Moussavi-Harami R. (2000) - Lithostratigraphic and facies analyses of the Sarcheshmeh Formation (Lower Cretaceous) in the eastern Kopet–Dagh Basin, NE Iran. *Cretaceous Res.*, 21: 507-516.

Roth P.H. (1978) - Cretaceous nannoplankton biostratigraphy and oceanography of the northwestern Atlantic ocean. In: Benson W.E. & Sheridan R.E. et al. - Initial Reports DSDP, 44: 731-759. Washington (U.S. Govt. Printing Office).

Seyed-Emami K. & Aryai A.A. (1981) - Ammoniten aus dem unteren Cenoman von Nordostiran (Koppeh-Dagh). *Mitt. Bayerischen Staat. Paläeontol. Histor. Geol.*, 21: 23-39.

Sissingh W. (1977) - Biostratigraphy of Calcareous. *Nannoplankton Geologie En Mijnbouw*, 56: 37-65.

Stocklin J. & Setudehnia A. (1991) - Stratigraphy Lexicon of Iran. *Geol. surv. Iran,* 18: 376.

Thibault N., Husson D., Harlou R., Gardin S., Galbrun B., Huret E. & Minoletti F. (2012) - Astronomical calibration of upper Campanian–Maastrichtian carbon isotope events and calcareous plankton biostratigraphy in the Indian Ocean (ODP Hole 762C): implication for the age of the Campanian–Maastrichtian boundary. *Palaeogeogr., Palaeoclimatol., Palaeoecol.,* 27: 1-68.

Vahidinia M. & Sadeghi A. (2011) - Lithostratigraphic and biostratigraphic studies of Nayzar Formation in Jalilabad section (North-west of Mashhad, Iran). 64thGeological Conference in Turkey, Abstracts: 251.

Watkins D.K. (2007) - Quantitative analysis of the calcareous nannofossil assemblages from CIROS-1, Victoria Land Basin, Antarctica. *J. Nannoplankton Res.*, 29(2): 130-137.
www.google.com/maps/@34.4952897,55.0062145,6z .

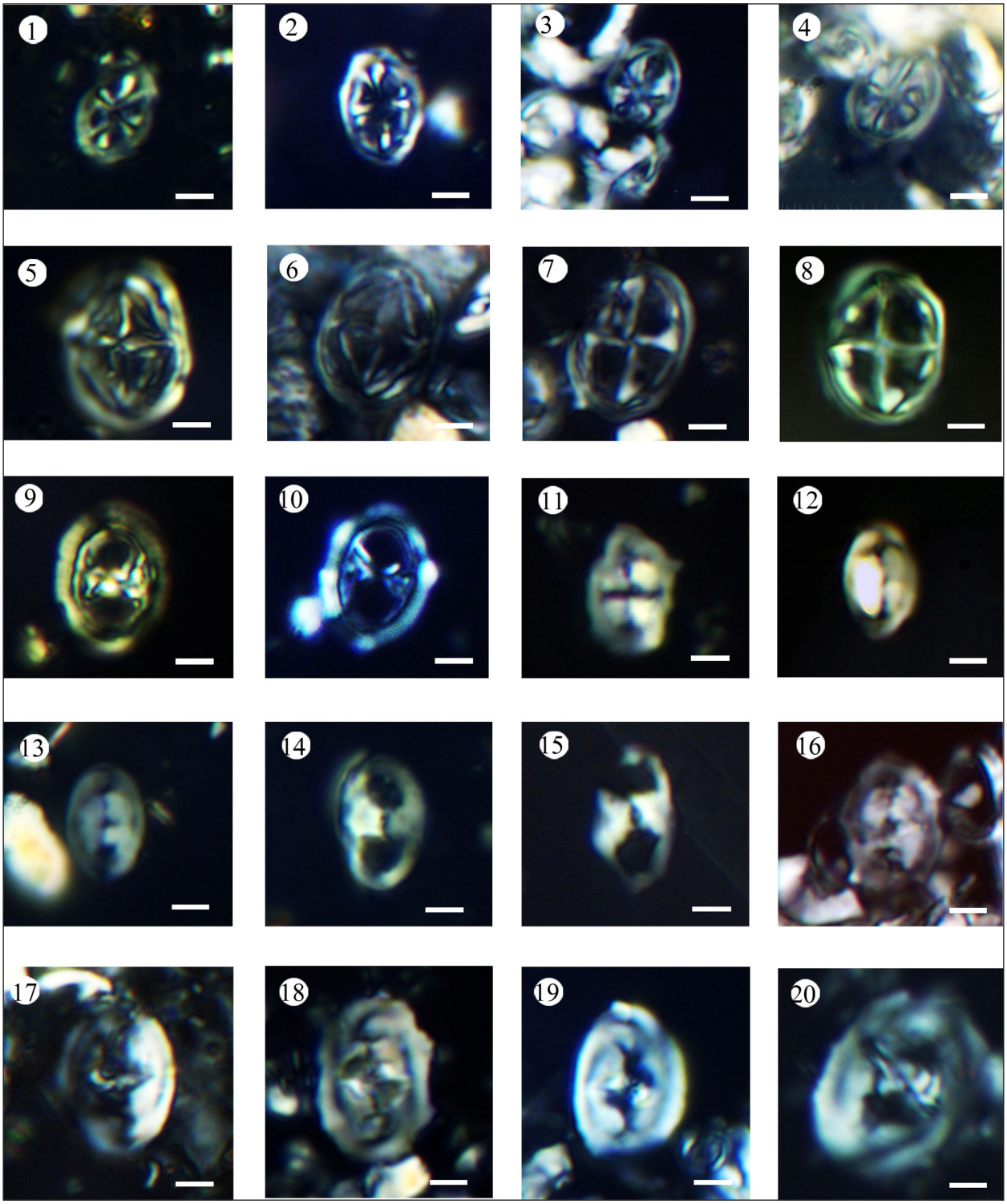

PLATE 1

Fig. 1 - *Ahmuellerella octoradiata*, (30° rotated), Sample No. FKB 130; Fig. 2 - *Ahmuellerella octoradiata*, Sample No. FPB 108; Fig. 3 - *Ahmuellerella regularis,* (30° rotated), Sample No. FPB 141; Fig. 4 - *Ahmuellerella regularis*, (40° rotated), Sample No. FPB 305; Fig. 5 - *Monomarginatus quaternarius*, Sample No. FJB 189; Fig. 6- *Monomarginatus quaternarius,* (30° rotated), Sample No. FKB 213; Fig. 7 - *Staurolithites mielnicensis*, (30° rotated), Sample No. FKB 126; Fig. 8 - *Staurolithites mielnicensis,* Sample No. FJB 161; Fig. 9 - *Amphizygus brooksii,* Sample No. FJB 189; Fig. 10 - *Amphizygus brooksii,* (30° rotated), Sample No. FPB 102; Fig. 11 - *Tranolithus orionatus*, Sample No. FJB 107; Fig. 12 - *Tranolithus orionatus*, Sample No. FJB 192; Fig. 13 - *Tranolithus orionatus*, Sample No. FPB 333; Fig. 14 - *Tranolithus gabalus*, Sample No. FKB 148; Fig. 15 - *Tranolithus gabalus*, Sample No. FPB 169; Fig. 16 - *Tranolithus orionatus*, Sample No. FKB 100; Fig. 17 - *Reinhardtites levis*, Sample No. FPB 338; Fig. 18 - *Reinhardtites anthophorus*, Sample No. FPB 103; Fig. 19 - *Reinhardtites* cf. *R. anthophorus,* (intermediate form between *R. anthophorus* and *R. levis*), Sample No. FPB 211; Fig. 20 - *Reinhardtites anthophorus*, (30° rotated), Sample No. FKB 107. Scale bar: 5 μm.

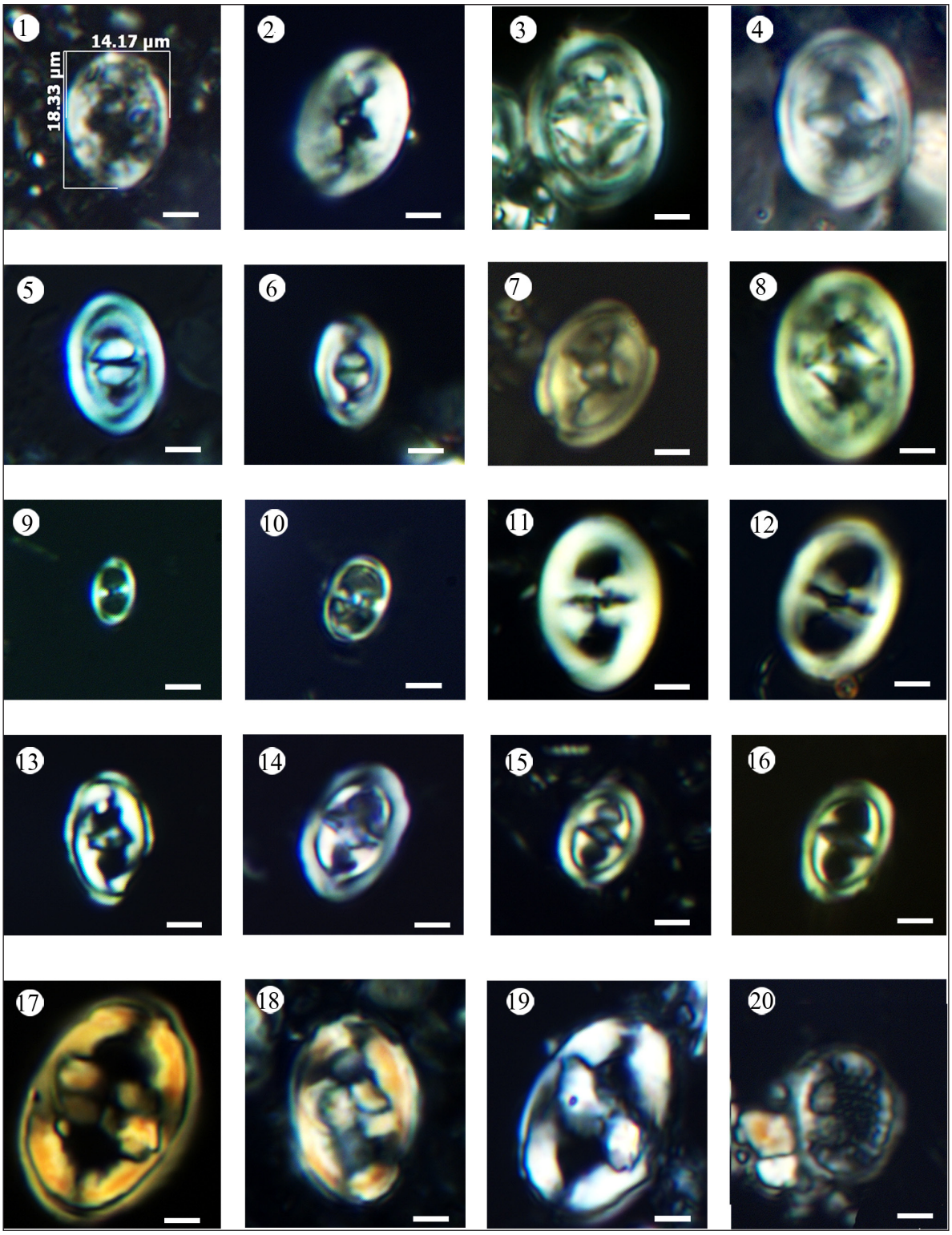

PLATE 2

Fig. 1- *Reinhardtites levis*, Sample No. FPB 138; Fig. 2 - *Reinhardtites levis*, Sample No. FKB 546; Fig. 3 - *Reinhardtites anthophorus*, Sample No. FPB 290; Fig. 4 - *Reinhardtites* cf. *R. levis,* (30º rotated),(intermediate form between *R. anthophorus* and *R. levis*), Sample No. FPB 353; Fig. 5 - *Zeugrhabdotus bicrescenticus,* Sample No. FKB 205; Fig. 6 - *Zeugrhabdotus bicrescenticus,* Sample No. FPB 333; Fig. 7 - *Reinhardtites levis,* Sample No. FKB 554; Fig. 8 - *Reinhardtites* cf. *R. levis*, Sample No. FJB 192; Fig. 9 - *Zeugrhabdotus erectus,* Sample No. FKB 345; Fig. 10 - *Zeugrhabdotus erectus,* (30º rotated), Sample No. FKB 455; Fig. 11 - *Zeugrhabdotus* cf. *Z. diplogramus,* Sample No. FKB 431; Fig. 12 - *Zeugrhabdotus* cf. *Z. diplogramus,* Sample No. FJB 299; Fig. 13 - *Zeugrhabdotus trivectis,* Sample No. FPB 211; Fig. 14 - *Zeugrhabdotus sigmoides,* (30º rotated), Sample No. FPB 300; Fig. 15 - *Zeugrhabdotus sigmoides,* (30º rotated), Sample No. FPB 346; Fig. 16 - *Zeugrhabdotus sigmoides,* (30º rotated), Sample No. FPB 282; Fig. 17 - *Zeugrhabdotus embergeri*, (30º rotated), Sample No. FKB 456; Figs. 18, 19 (30º rotated)- *Zeugrhabdotus embergeri,* Sample No. FKB 173; Fig. 20 - *Cribrosphaerella ehrenbergii,* Sample No. FPB 102. Scale bar: 5 µm.

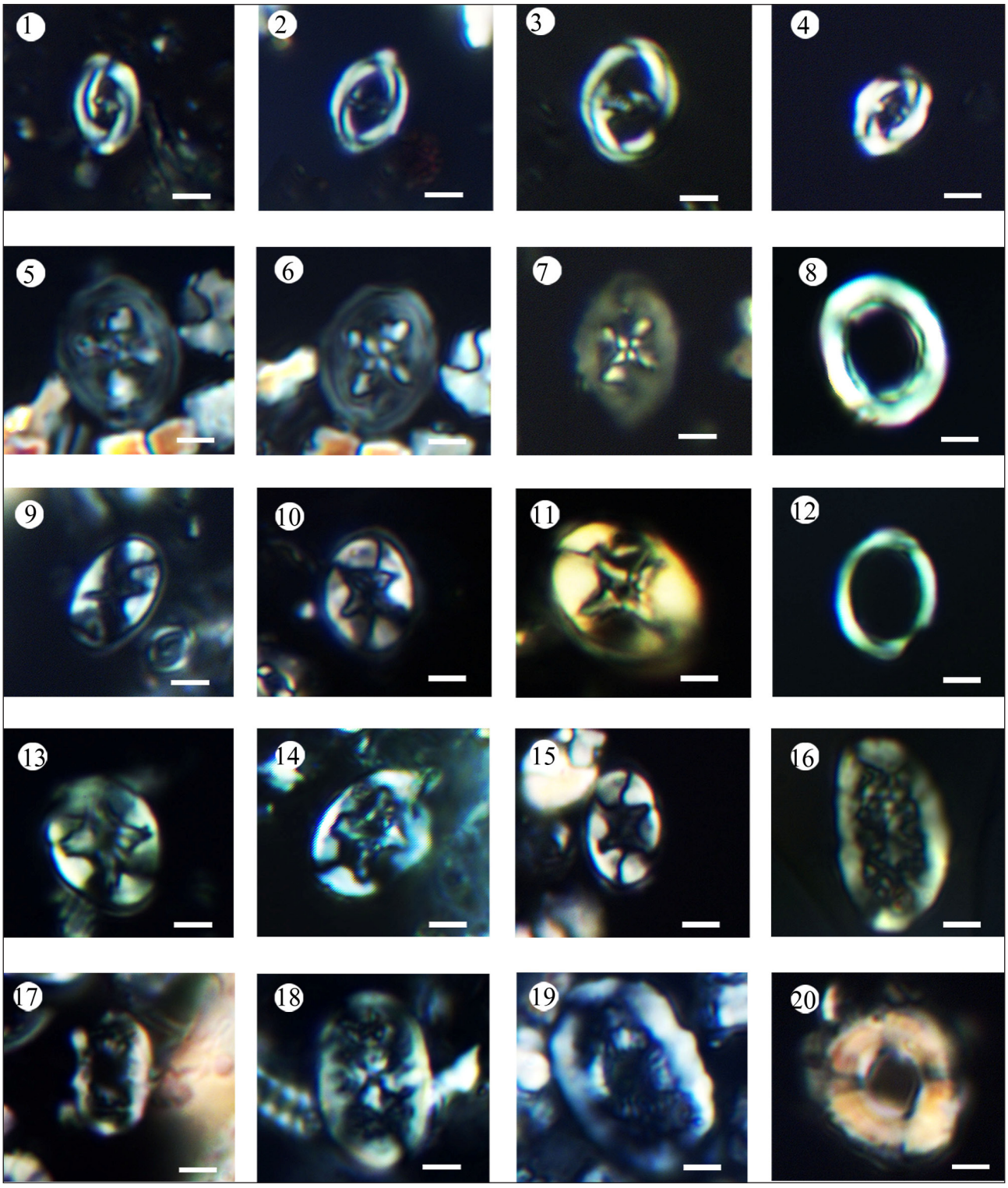

PLATE 3

Fig. 1- *Placozygus fibuliformis,* Sample No. FKB 141; Fig. 2 - *Placozygus fibuliformis,* (30° rotated), Sample No. FPB 103; Fig. 3 - *Placozygus fibuliformis,* (15° rotated), Sample No. FPB 189; Fig. 4 - *Placozygus fibuliformis,* (40° rotated), Sample No. FPB 239; Fig. 5 - *Chiastozygus litterarius,* Sample No. FPB 104; Fig. 6 - *Chiastozygus litterarius,* (30° rotated), Sample No. FPB 104; Fig. 7 - *Chiastozygus litterarius,* Sample No. FPB 102; Fig. 8 - *Loxolithus armilla*, (30° rotated), Sample No. FKB 345; Fig. 9 - *Eiffellithus gorkae*, (30° rotated), Sample No. FPB 145; Fig.10 - *Eiffellithus turriseiffelii,* Sample No. FKB 130; Fig. 11 - *Eiffellithus turriseiffelii,* (45° rotated), Sample No. FPB 152; Fig.12 - *Loxolithus armilla*, Sample No. FKB 345; Fig. 13 - (10° rotated), *Eiffellithus parallelus*, Sample No. FPB 343; Fig. 14 - *Eiffellithus parallelus*, (30° rotated), Sample No. FKB 300; Fig. 15 - *Eiffellithus turriseiffelii*, Sample No. FPB 134; Fig. 16 - *Rhagodiscus reniformis,* Sample No. FPB 204; Fig. 17 - *Rhagodiscus splendens*, Sample No. FPB 134; Fig. 18 - *Rhagodiscus splendens,* Sample No. FKB 168; Fig. 19 - *Rhagodiscus splendens,* (30° rotated), Sample No. FKB 111; Fig. 20 - *Cylindrolithus sculptus*, Sample No. FPB 279. Scale bar: 5 μm.

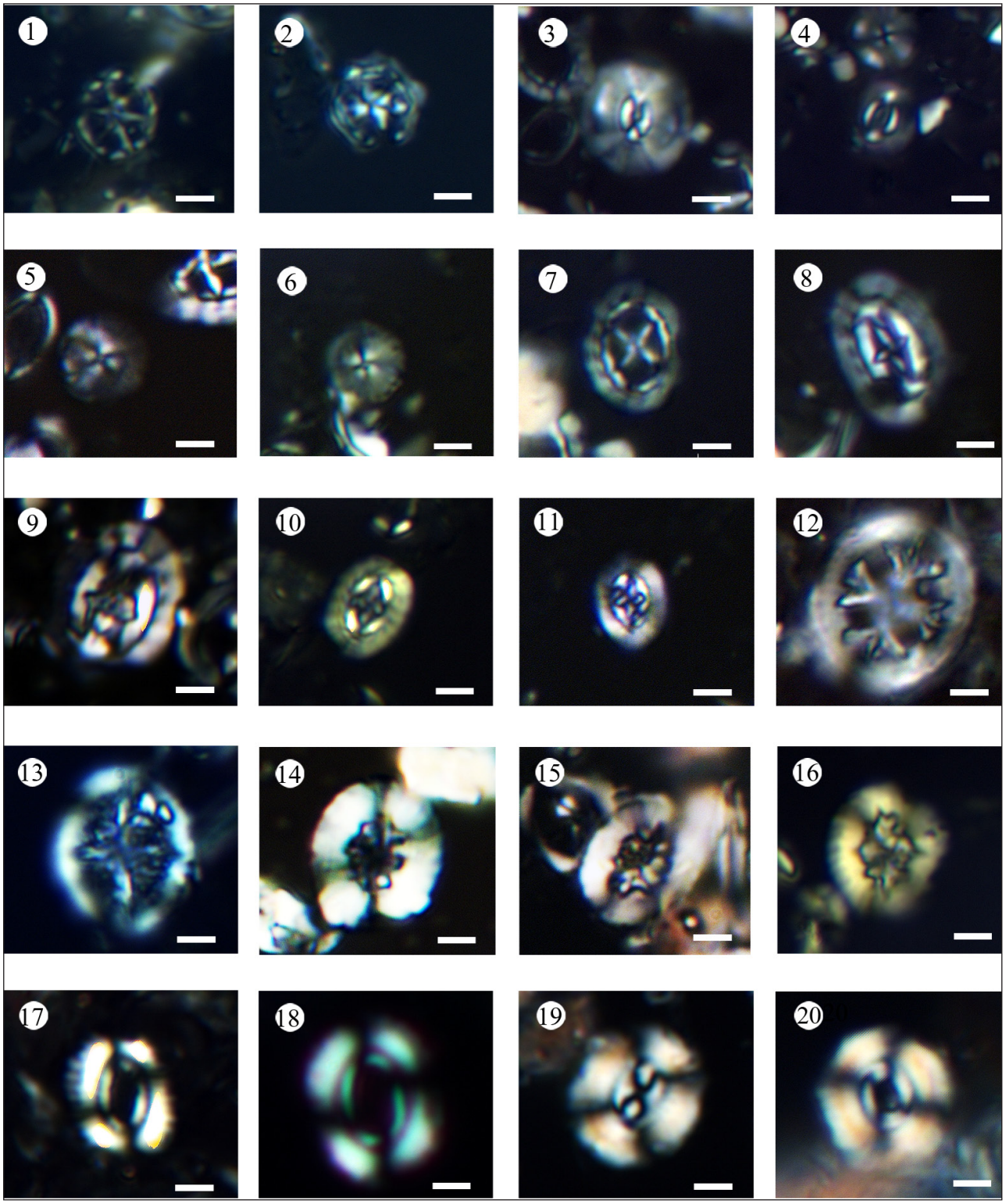

PLATE 4

Fig. 1 - *Corollithion exiguum*, Sample No. FPB 148; Fig. 2 - *Corollithion exiguum,* Sample No. FKB 205; Fig. 3 - *Biscutum elliplicum*, (5º rotated), Sample No. FKB 100; Fig. 4 - *Biscutum ellipticum,* (20º rotated), Sample No. FPB 134; Fig. 5 - *Discorhabdus ignotus*, Sample No. FKB 130; Fig. 6 - *Discorhabdus ignotus*, Sample No. FPB 157; Fig. 7 - *Prediscosphaera cretacea,* Sample No. FPB 302; Fig. 8 - *Prediscosphaera arkhangelskyi,* (30º rotated), Sample No. FKB 271; Fig. 9 - *Prediscosphaera arkhangelskyi,* Sample No. FPB 137; Fig. 10 - *Prediscosphaera stoveri*, (30º rotated), Sample No. FKB 455; Fig.11 - *Prediscosphaera stoveri*, Sample No. FPB 300; Fig.12 - (30º rotated), *Retecapsa schizobrachiata*, Sample No. FKB 186; Fig. 13- *Cretarhabdus conicus*, Sample No. FPB 209; Fig. 14 - *Retecapsa angustiforata,* Sample No. FPB 102; Fig. 15 - *Retecapsa* cf. *R. crenulata*, (3 0º rotated), Sample No. FPB 133; Fig. 16 - *Retecapsa angustiforata*, Sample No. FKB 455; Fig. 17 - *Watznaueria ovata*, Sample No. FPB 352; Fig. 18 - *Watznaueria ovata*, Sample No. FPB 353; Fig. 19 - *Watznaueria barnesiae,* Sample No. FKB 100; Fig. 20 - *Cyclagelosphaera* sp., Sample No. FPB 145. Scale bar: 5 µm.

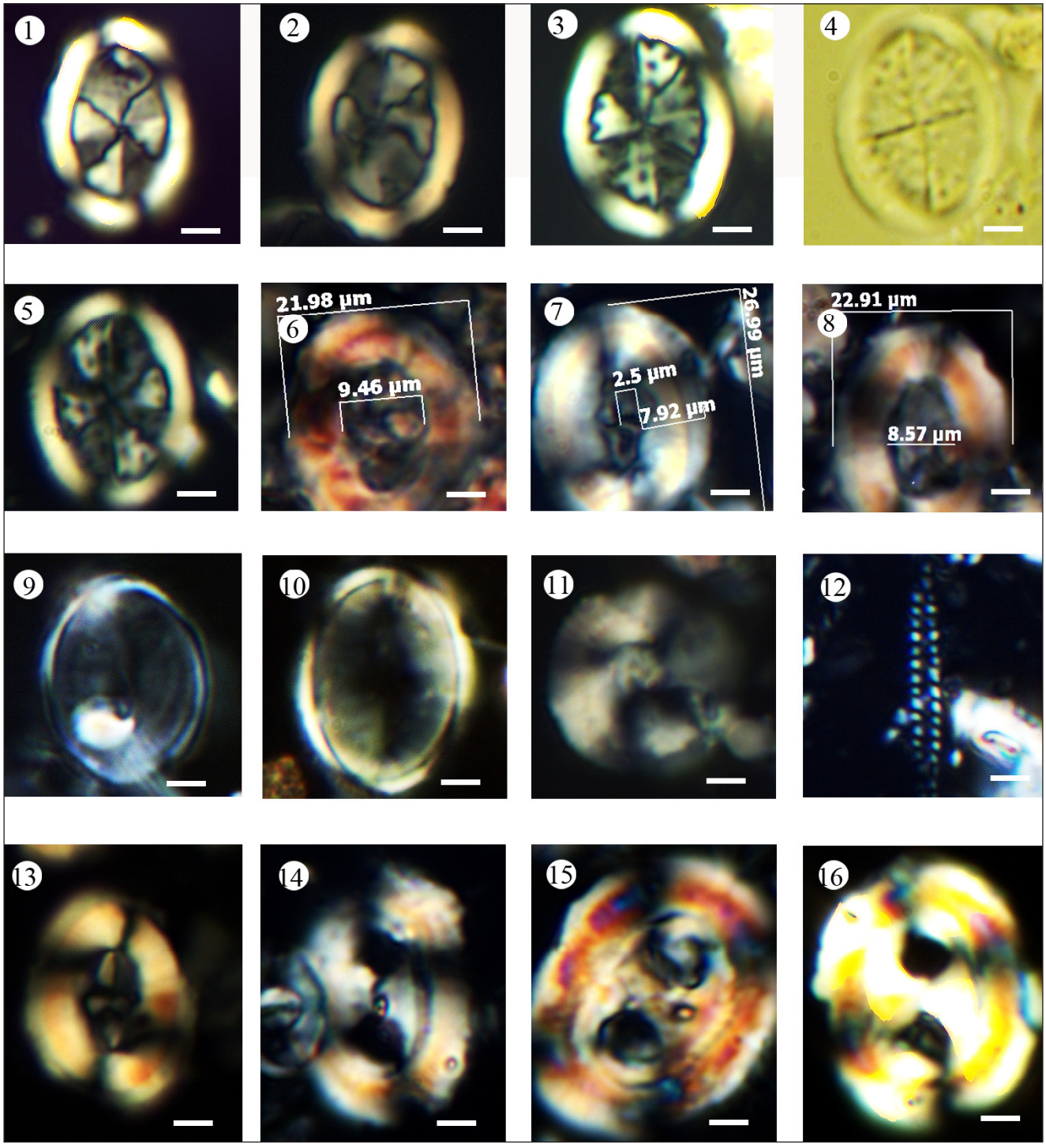

PLATE 5

Fig. 1 - *Arkhangelskiella cymbiformis,* Sample No. FKB 148; Fig. 2 - *Arkhangelskiella cymbiformis,* (15° rotated),Sample No. FPB 168; Fig. 3 - *Arkhangelskiella specillata*, (5° rotated), Sample No. FJB 189; Fig. 4 - *Arkhangelskiella specillata*, (BF), Sample No. FJB 189; Fig. 5 - *Arkhangelskiella cymbiformis,* Sample No. FPB 346; Fig. 6 - *Broinsoniaparcaparca,* Sample No. FPB 108; Fig. 7 - *Broinsonia parca constricta,* Sample No. FKB 126; Fig. 8 - *Broinsoniaparcaparca*, Sample No. FPB 110; Fig. 9 - *Kamptnerius magnificus*, Sample No. FPB 348; Fig. 10 - *Kamptnerius magnificus,* Sample No. FPB 108; Fig. 11 - *Haqius circumradiatus,* Sample No. FKB 256; Fig. 12 - *Microrhabdulus belgicus,* Sample No. FPB 180; Fig. 13 - *Broinsoniaparcaparca,* Sample No. FKB 105; Fig. 14 - *Watznaueria biporta,* Sample No. FPB 180; Fig. 15 - *Watznaueria biporta,*(25° rotated), Sample No. FPB 173; Fig. 16 - *Watznaueria biporta,* Sample No. FKB 299. Scale bar: 5 µm.

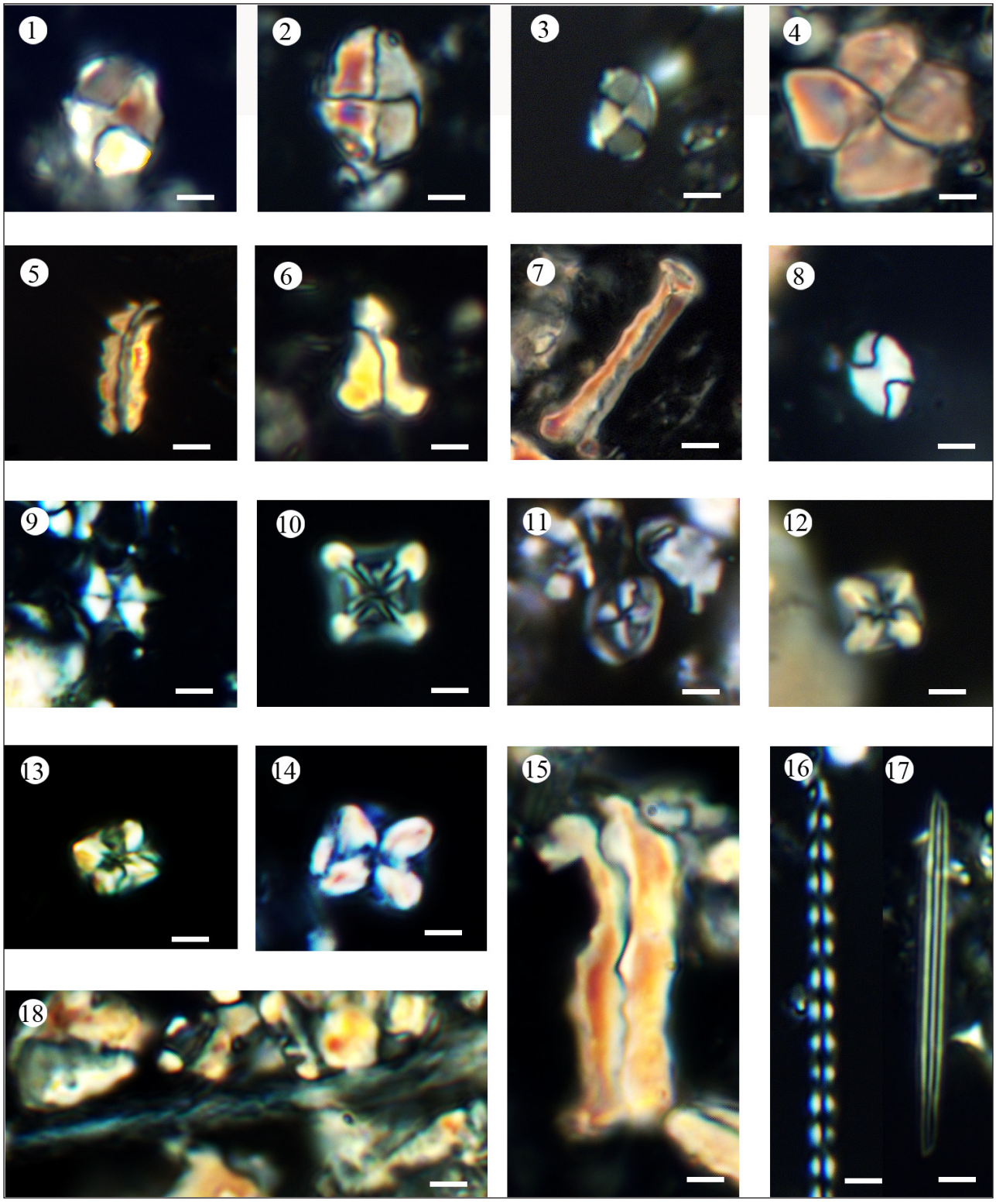

PLATE 6

Fig. 1 - *Calculites obscurus*, Sample No. FPB 324; Fig. 2 - *Calculites ovalis,* Sample No. FPB 102; Fig. 3 - *Calculites obscurus*, Sample No. FKB 148; Fig. 4 - *Petrarhabdus copulatus*, Sample No. FPB 324; Fig. 5 - *Lucianorhabdus cayeuxii*, Sample No. FPB 342; Fig. 6 - *Lucianorhabdus maleformis*, Sample No. FPB 318; Fig. 7 - *Lucianorhabdus arcuatus*, Sample No. FPB 125; Fig. 8 - *Calculites obscurus*, (30º rotated), Sample No. FPB 301; Fig. 9 - *Lithastrinus grillii*, Sample No. FPB 343; Fig. 10 - *Quadrum svabenickae*, Sample No. FKB 400; Fig. 11 - *Gartnerago segmentatum*, Sample No. FPB 153; Fig. 12 - *Micula decussata*, Sample No. FPB 302; Fig. 13 - *Micula decussata*, Sample No. FJB 198; Fig. 14 - *Micula decussata,* Sample No. FPB 209; Fig. 15 - *Lucianorhabdus cayeuxii*, Sample No. FPB 352, Fig. 16 - *Microrhabdulus decoratus*, Sample No. FPB 193; Fig. 17 - *Lithraphidites carniolensis*, Sample No. FKB 437; Fig. 18 - *Micorhabdulinus ambiguus* (curved spine), Sample No. FPB 157. Scale bar: 5 µm.

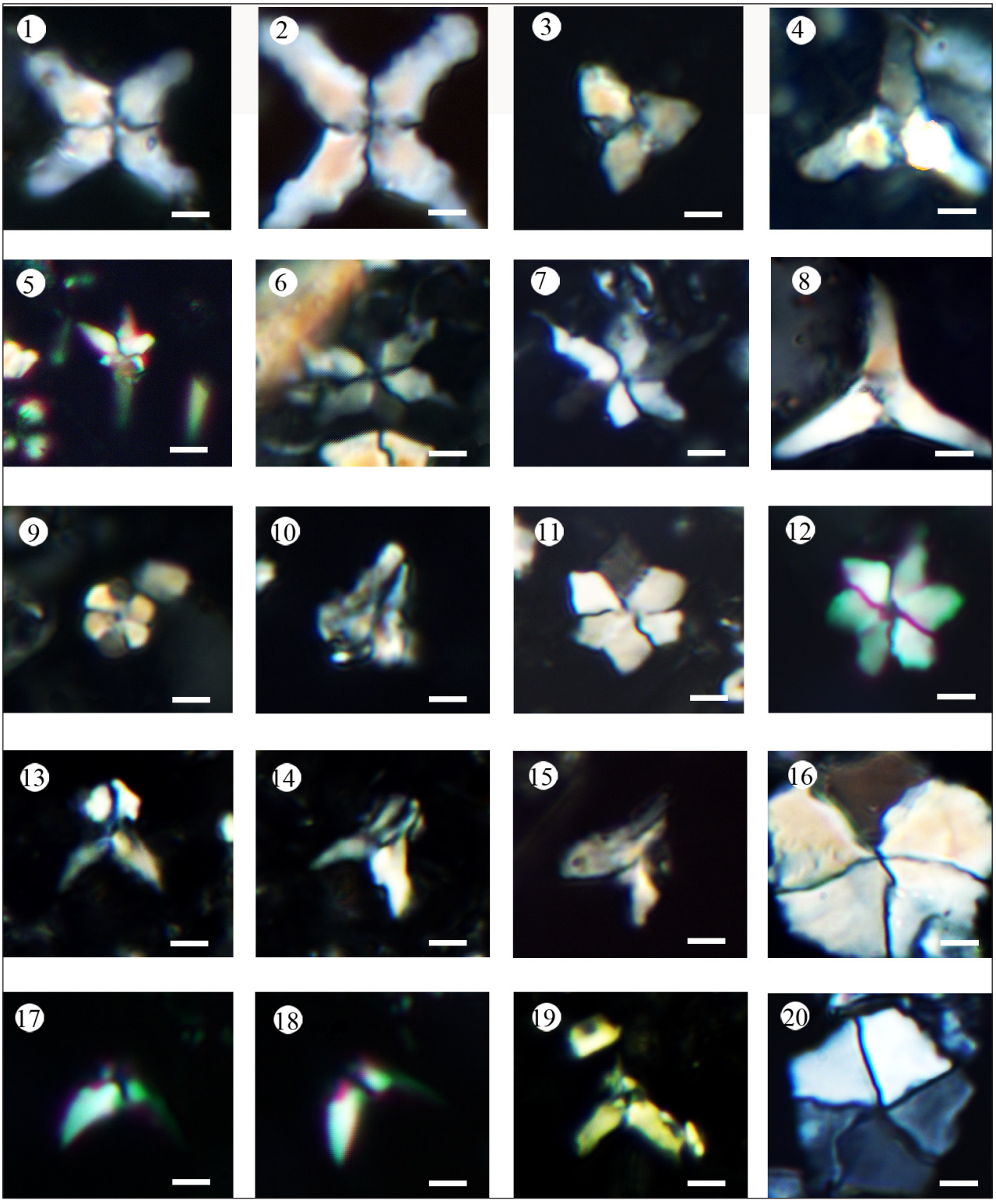

PLATE 7

Fig. 1 - *Uniplanarius sissinghii,* Sample No. FPB 134; Fig. 2 - *Uniplanarius sissinghii,* Sample No. FPB 343; Fig. 3 - *Uniplanarius trifidus*, (wide and short rays) Sample No. FPB 315; Fig. 4 - *Uniplanarius trifidus*, (narrow and tall rays), Sample No. FKB 160; Fig. 5 - *Rucinolithus hayi,* Sample No. FPB 348; Fig. 6 - *Rucinolithus magnus,* Sample No. FPB 290; Fig. 7 - *Rucinolithus magnus*, Sample No. FPB 300; Fig. 8 - *Uniplanarius trifidus*, (narrow and tall rays), Sample No. FKB 556; Fig. 9 - *Hexalithushexalithus*, Sample No. FPB 333. Fig. 10 - *Ceratolithoides verbeekii*, Sample No. FPB 103; Fig. 11 - *Rucinolithus hayi,* Sample No. FPB 305; Fig. 12 - *Rucinolithus hayi,* Sample No. FPB 352; Fig. 13 - *Ceratolithoides* cf. *C. aculeus,* Sample No. FPB 214; Fig. 14 - *Ceratolithoides* cf. *C. aculeus,* (30º rotated), Sample No. FPB 214; Fig. 15 - *Ceratolithoides aculeus*, (30º rotated), Sample No. FPB 141; Fig. 16 - *Braarudosphaera bigelowii*, Sample No. FPB 168; Fig. 17, 18 (30º rotated) - *Ceratolithoides arcuatus*, Sample No. FPB 348; Fig. 19 - *Ceratolithoides arcuatus*, Sample No. FKB 271; Fig. 20 - *Braarudosphaera bigelowii*, Sample No. FKB 130. Scale bar: 5 µm.

Appendix
Taxonomic index

Alphabetical list of calcareous nannofossil species cited in the text, figures 1 to 6, plates 1 to 7 and tables 1 to 3. Most bibliographic references can be found in Perch-Nielsen (1985) and Bown (1998) and Lees & Bown (2005).

References not cited in this paper can be found in Perch-Nielsen (1985), Bown (1998) and Lees & Bown (2005).

Ahmuellerella octoradiata (Górka, 1957) Reinhardt, 1966.
Ahmuellerella regularis (Gorka, 1957) Reinhardt & Gorka, 1967.
Amphizigus brooksii Bukry, 1969.
Arkhangelskiella cymbiformis Vekshina, 1959.
Arkhangelskiella specillata Vekshina, 1959.
Biscutum constans (Górka, 1957) Black, 1959.
Biscutum magnum Wind and Wise in Wise & Wind, 1977.
Biscutum ellipticum (Górka, 1957) Griin in Griin & Allemann, 1975.
Braarudosphaera bigelowii (Gran & Braarud, 1935) Deflandre, 1947.
Broinsonia parca parca (Stradner, 1963) Bukry, 1969.
Broinsonia parca constricta Hattner et al., 1980.
Calculites obscurus (Deflandre, 1959) Prins & Sissingh in Sissingh, 1977.
Calculites ovalis (Stradner, 1963) Prins & Sissingh in Sissingh, 1977.
Ceratolitoides aculeus (Stradner, 1961) Prins & Sissingh in Sissingh, 1977.
Ceratolitoides arcuatus Prins & Sissingh in Sissingh, 1977.
Ceratolithoides verbeekii Perch-Nielsen, 1979.
Chiastozygus litterarius (Górka, 1957) Manivit, 1971.
Corollithion exiguum Stradner, 1961.
Cretarhabdus conicus Bramlette & Martini, 1964.
Cribrosphaerella ehrenbergii (Arkhangelsky, 1912) Deflandre in Pivetteau, 1952.
Cyclagelosphaera sp. Bukry, 1969.
Discorhabdus ignotus (Górka, 1957) Perch-Nielsen, 1968.
Eiffellithus eximius (Stover, 1966) Perch-Nielsen, 1968.
Eiffellithus parallelus Perch-Nielsen, 1973.
Eiffellithus gorkae Reinhardt, 1965.
Eiffellithus turriseiffelii (Deflandre in Deflandre & Fert, 1954) Reinhardt, 1965.
Grantarhabdus coronadventis (Reinhardt, 1966) Grun in Grun & Allemann, 1975.
Haqius circumradiatus (Stover, 1966) Roth, 1978.
Hexalithus hexalithus Gradet, 1955 in Perch-Nielsen, 1984.
Kamptnerius magnificus Deflandre, 1959.
Lithastrinus grillii Stradner, 1962.
Lithraphidites carniolensis Deflandre, 1963.
Loxolithus armilla (Black in Black & Barnes, 1959) Noel, 1965.
Lucianorhabdus arcuatus Forchheimer 1972.
Lucianorhabdus cayeuxii Deflandre, 1959.
Lucianorhabdus maleformis Reinhardt, 1966.
Microrhabdulus belgicus Haye & Towe, 1963.
Microrhabdulus decoratus Deflandre, 1959.
Microrhabdulus undosus Perch-Nielsen ,1973.
Micorhabdulinus ambiguus (curved spine) Deflander, 1963.
Micula concava (Stradner in Martini & Stradner, 1960) Verbeek, 1976.
Micula decussata Vekshina, 1959.
Misceomarginatus pleniporus Wind & Wise and Wise & Wind, 1977.
Monomarginatus quaternarius Wind & Wise in Wise & Wind, 1977.
Petrarhabdus copulatus (Deflandre, 1959) Wind & Wise in Wise, 1983.
Prediscosphaera arkhangelskyi (Reinhardt, 1965) Perch-Nielsen, 1984.
Prediscosphaera cretacea (Arkhangelsky, 1912) Gartner, 1968.
Prediscosphaera stoveri (Perch-Nielsen, 1968) Shafik & Stradner, 1971.
Quadrum gartneri Prins & Perch-Nielsen in Manivit et al., 1977.
Quadrum svabenickae Burnett, 1998b.
Reinhardtites anthophorus (Deflandre, 1959) Perch-Nielsen, 1958.
Reinhardtites levis Prins & Sissingh in Sissingh, 1977.
Retecapsa angustiforata Black, 1971a.
Retecapsa crenulata (Bramlette & Martini, 1964) Grun in Grun & Allemann, 1975.
Retecapsa ficula (Stover, 1966) Burnett, 1998b.
Retecapsa schizobrachiata (Gartner, 1968) Grun in Grun & Allemann, 1975.
Rhagodiscus angustus (Stradner, 1963) Reinhardt, 1971.
Rhagodiscus reniformis Perch-Nielsen, 1973.
Rhagodiscus splendens (Deflander, 1953) Verbeek, 1977.
Rucinolithus hayi Stover, 1966.
Rucinolithus magnus Bukry, 1975.
Staurolithites mielnicensis (Gorka, 1957) Perch-Nielsen, 1968 sensu Crux in Lord, 1982.
Tranolithus orionatus (Reinhardt, 1966a) Reinhardt, 1966b.
Tranolithus phacelosus Stover 1966.
Uniplanarius sissinghii Perch-Nielsen, 1986b.
Uniplanarius trifidus (Stradner in Stradner & Papp, 1961) Hattner & Wise, 1989.
Watznaueria barnesiae (Black, 1959) Perch-Nielsen, 1968.
Watznaueria biporta Bukry 1969.
Watznaueria ovata Bukry, 1969.
Zeugrhabdotus bicrescenticus (Stover, 1966) Burnett in Gale et al., 1996.
Zeugrhabdotus embergeri (Noël, 1958) Perch-Nielsen, 1984
Zeugrhabdotus erectus (Deflandre in Deflandre & Fert, 1954) Reinhardt, 1965.
Zeugrhabdotus sigmoides (Bramlette & Sullivan, 1961) Bown & Young, 1997.
Zeugrhabdotus trivectis Bergen, 1994.